HHS Public Access

Author manuscript

Int J Radiat Oncol Biol Phys. Author manuscript; available in PMC 2023 July 01.

Published in final edited form as:

Int J Radiat Oncol Biol Phys. 2022 July 01; 113(3): 624–634. doi:10.1016/j.ijrobp.2022.03.016.

Ultrafast Tracking of Oxygen Dynamics during Proton FLASH

Mirna El Khatib, PhD[a,*], **Alexander L. Van Slyke, PhD**[b,*], **Anastasia Velalopoulou, PhD**[b], **Michele M. Kim, PhD**[b], **Khayrullo Shoniyozov, PhD**[b], **Srinivasa Rao Allu, PhD**[a], **Eric E. Diffenderfer, PhD**[b], **Theresa M. Busch, PhD**[b], **Rodney D. Wiersma, PhD**[b], **Cameron J. Koch, PhD**[b], **Sergei A. Vinogradov, PhD**[a]

[a]Department of Biochemistry and Biophysics, Perelman School of Medicine, and Department of Chemistry, School of Arts and Sciences, University of Pennsylvania, Philadelphia, PA 19104

[b]Department of Radiation Oncology, Perelman School of Medicine, University of Pennsylvania, Philadelphia, PA 19104

Abstract

Purpose: Radiation therapy delivered at ultrafast dose rates, known as FLASH RT, has been shown to provide a therapeutic advantage compared to conventional radiotherapy by selectively protecting normal tissues. Radiochemical depletion of oxygen has been proposed to underpin the FLASH effect, however experimental validation of this hypotheses has been lacking, in part due to the inability to measure oxygenation at rates compatible with FLASH.

Methods and Materials: We present a new variant of the phosphorescence quenching method for tracking oxygen dynamics with rates reaching up to ~3.3 kHz. Using soluble Oxyphor probes we were able to resolve, both *in vitro* and *in vivo*, oxygen dynamics during the time of delivery of proton FLASH.

Results: (1) *In vitro* in solutions containing bovine serum albumin (BSA) the O_2 depletion *g*-values (moles/L of O_2 depleted per radiation dose, e.g. μM/Gy) are higher for conventional irradiation (by ~13% at 75 μM [O_2]) than for FLASH, and in the low-oxygen region (<25 μM [O_2]) they decrease with oxygen concentration. (2) *In vivo*, depletion of oxygen by a single FLASH is insufficient to achieve severe hypoxia in initially well-oxygenated tissue; and (3) the *g*-values measured appear to correlate with baseline oxygen levels.

Conclusions: The developed method should be instrumental in radiobiological studies, such as studies aimed at unraveling the mechanism of the FLASH effect. The FLASH effect could in part

Corresponding authors Sergei A. Vinogradov, PhD, vinograd.upenn@gmail.com, Cameron J. Koch, PhD, kochc@pennmedicine.upenn.edu.
*Equal contributions.

Conflict of Interest Notification

S.A.V. has partial ownership of Oxygen Enterprises Ltd, which owns the intellectual property for phosphorescent probes technology (US Pat. No. 9,556,213; US, 2017/0137449 A1). All other authors declare no competing interests

Data sharing statement

All data generated and analyzed during this study are included in this published article (and its Supporting information).

originate from the difference in the oxygen dependencies of the oxygen consumption *g*-values for conventional *vs* FLASH RT.

Keywords

phosphorescence quenching; oxygen; proton radiotherapy; FLASH radiotherapy; Oxyphor

Introduction

It has been known for a long time that radiation delivered at ultrahigh dose rates can result in less damage to cells compared to conventional delivery, which relies on rates that are hundreds of times lower.[1–3] Recent studies have shown that radiotherapy (RT) utilizing ultrahigh does rates (>40 Gy/s), known as FLASH RT,[4,5] is capable of more selective sparing of normal tissues, while maintaining tumor-control and thus improving the therapeutic ratio.[6–14] However, despite the potential of FLASH RT, the underpinning physical chemistry and biology of the FLASH effect remain unknown. Several hypotheses have been put forward to explain the enhanced specificity of FLASH RT,[12,15–17] among which the so-called oxygen depletion hypothesis[15] is being extensively discussed in the literature.[18–22] This hypothesis builds upon the fact that normally oxygenated tissues exhibit significantly higher radiosensitivity than tissues in the state of hypoxia *via* the so-called oxygen enhancement effect.[23] It has been suggested that fast and profound depletion of oxygen by FLASH in normal tissues facilitates their radioresistance, while in tumors, which are presumed to be hypoxic from the onset, changes in oxygen are relatively small and thus have lesser impact on radiosensitivity.

Several recent reviews[5,21,24] have pointed out that one of the stumbling points in testing the oxygen depletion hypothesis has been the difficulty in measuring rapid changes in tissue oxygenation inflicted by FLASH. Oxygen electrodes and approaches based on imaging of hypoxia markers do not possess the required temporal resolution, since re-oxygenation of tissue upon application of FLASH may occur just in fractions of a second.[25] In contrast, optical methods based on phosphorescence quenching can be tailored for the task, and their use has been encouraged.[21]

There exist two variants of the phosphorescence-based oximetry. In the first, phosphorescent chromophores are dissolved in solid polymers, and the resulting membranes are either attached to the tips of optical fibers or inserted directly into the measurement medium and probed in non-contact fashion. Solid-state technology has been extensively reviewed[26] and is available from a number of commercial sources. While straightforward in implementation, this approach is not appropriate for measurements *in vivo*, as insertion of a solid device into tissue inevitably leads to its damage and profoundly alters oxygenation.

The second approach, which is known as the phosphorescence quenching method,[27,28] makes use of soluble probes, which are injected directly into tissue, and the signals are obtained using external detectors and excitation sources, thereby permitting essentially non-invasive measurements of oxygenation. With appropriately designed molecular probes[29,30] phosphorescence is highly selective for oxygen, and because oxygen levels are derived from phosphorescence decay times (lifetimes), measurements are independent of the probe

concentration. Implementations of the method range from fiber-optic oximetry[31,32] to high-resolution microscopy[33,34] to different forms of imaging.[28,35–37]

Recently, Cao et al have used the phosphorescence quenching method to monitor oxygen changes upon application of electron FLASH *in vitro* and *in vivo*.[38] However, the temporal resolution of the reported experiments did not exceed ~7 Hz due to the limitations of instrumentation. This rate was adequate for quantifying oxygenation before and after FLASH, but insufficient for resolving oxygen dynamics during the time of irradiation. Nevertheless, the results implied that depletion of oxygen by a single electron FLASH is much less than necessary to achieve global hypoxia.

In an independent study Jansen et al performed oxygen measurements in pure water subjected to different types of radiation using a commercial solid-state phosphorescent sensor.[39] Temporal resolution of solid sensors (2.5 Hz in ref. [39]) is limited by the time required for oxygen to equilibrate between the measurement medium (water) and the polymeric membrane supporting the phosphorescent dye. Furthermore, the mechanisms of radiochemical consumption of oxygen in pure water and in media containing organic molecules, such as the biological milieu, are significantly different,[21] while the polymer membrane might have its own effect on the local oxygen depletion.

The above experiments provided valuable insights; however, they were unable to assess the dynamics of oxygen *in vivo* during the actual time of FLASH irradiation, and the question as to whether FLASH is able to achieve a transient state of deep hypoxia remained open, notwithstanding several modeling studies that argued against the oxygen depletion hypothesis.[16,40] Herein, we report a new implementation of the phosphorescence-quenching method that allowed us to perform oxygen measurements with temporal resolution reaching up to several kHz, which is hundreds of times faster than reported previously. Using this method we monitored changes in oxygenation continuously from the start to the end of proton FLASH, proving that a single clinical radiation dose applied to normally oxygenated tissue is unlikely to induce the state of severe hypoxia. Furthermore, we observed a dependence of the oxygen depletion *g*-values on the baseline oxygen levels, which may be relevant to the mechanism of the FLASH effect. The physical chemistry of phosphorescence-based measurements during application of radiation is discussed with the purpose to define the method's applicability limits in radiation biology studies.

Methods and Materials

Proton RT

The proton beam (230 MeV) was derived from a commercial cyclotron system (IBA Proteus Plus, Louvain-La-Neuve, Belgium), with protons delivered as 2 ns-long pulses at the repetition rate of 106 MHz. Considering the rates of the chemical processes relevant to this study, a beam with such temporal structure can be considered a continuous-wave source. The beam was collimated to 26 mm using a double-scattering collimator, and its profile and alignment were verified using a Gafchromic EBT3 dosimetry film (Ashland Advanced Materials, Bridgewater, NJ). For all irradiations the alignment of the target was performed using external lasers, which provided vertical and horizontal lines crossing at

the beam isocenter. The dose rate at the isocenter was measured prior to each experiment using a NIST-traceable Advanced Markus parallel plate chamber (PTW, Freiburg, Germany), equipped with a digital oscilloscope. The beam collimator, the samples and the measurement equipment were positioned in a shielded vault (treatment room). Beam delivery and measurements were controlled remotely.

Phosphorescence measurements

Oxygen measurements were performed using a molecular water-soluble probe Oxyphor PtG4[30,37,41] and a fiber-optic phosphorometer (*Oxyled*, Oxygen Enterprises; SI, p. S4). The phosphorescence lifetime of PtG4 in aqueous media in the absence of oxygen (τ_0) is 51 μs at 23°C and 49.5 μs at 37°C. The probe's response to oxygen was calibrated as described previously.[41] In addition, two probes Oxyphor PdG4[41] and Oxyphor 2P[42] have been employed in several experiments.

In the *Oxyled* system, a single data acquisition cycle (T) consists of an excitation pulse (δt) and the phosphorescence collection period (Δt). Usually, multiple (N) cycles are executed in sequence, the resulting data array is transferred to the host computer, decays are averaged and fitted to a single-exponential (or another suitable model) using the non-linear least squares method. The obtained decay time τ (lifetime) is converted to oxygen concentration using an empirical Stern-Volmer-like relationship, known from independent calibrations.[41]

A measurement consisting of e.g. N=10 cycles of duration T=300 μs (appropriate for experiments with Oxyphor PtG4) requires 3 ms with additional 5–10 ms for data transfer and analysis. However, due to the internal operation of the hardware, the maximal measurement rate achievable with commercial instrumentation is ~7 Hz (~150 ms per measurement). A custom program was written (C/C++, Qt, Nokia), which allowed us to execute measurement cycles continuously with the data being transferred to the host memory in parallel with execution. As a result, the duration of the recording was limited only by the memory on the computer and could be many seconds-long without reducing the sampling frequency. If proton FLASH was delivered during the recording, its effect on the phosphorescence was captured within the data array. Provided that the SNR of each individual decay was sufficient to determine its time constant, oxygen sampling was performed with the repetition rate 1/T, 3.33 kHz. Additionally, algorithms were developed to deal with effects of radiation on the detector and to reduce noise (see Results).

Samples for in vitro experiments

A solution of the probe (~2 μM) in distilled water deionized water (Milli-Q) or in a buffer (20 mM phosphate, pH 7.2) containing bovine serum albumin (Sigma) was placed in a cylindrical glass vial (5 mL) with a screw cap (Fisherbrand™ Class B Clear Glass, diameter 15 mm, length 45 mm), such that no air bubbles remained in the vial after sealing the cap. The vial was placed in a cylindrical hole drilled in an polyacrylic block (see SI, p.S3), such that the proton beam was directed onto the vial cap, and the vial's axis was collinear with the beam. The beam diameter was 26 mm, so that the entire vial was exposed to the radiation. The optical fibers were inserted through a channel perpendicular to the beam axis. The fibers' tips were positioned next to the vial ~1.5 cm from the beam entry into the vial. Thus,

a ~5–7 mm-thick slab of the solution contributed to the sampled data. It was confirmed in separate experiments that there was no diffusion of oxygen from the air into the sealed vials.

In vivo experiments

The animal studies were approved by the Institutional Animal Care and Use Committee. Eight-to-ten weeks-old C57Bl/6 mice (Jackson Labs) were injected with solution of Oxyphor PtG4 (100 μM, 20 μL) into the leg muscle of the right hind leg 24h before irradiation and measurements. The probe distributed through the interstitial space in the muscle. Previous experiments have shown that upon interstitial delivery of the probes signals can be collected from the tissue for days following the injection.[41,42] Introducing a waiting period (24h) between the injection and the measurements allowed the wound from the needle to heal, bringing the oxygen levels around the injection site back to normal. During the measurements mice were anesthetized (isofluorane in air, 1.5–2%, administered *via* inhalation through a nose cone). The right hind leg of the mouse was positioned such that the beam isocenter was approximately at the center of the desired irradiated area, and a single dose of proton radiation (30 Gy) was delivered at a FLASH rate. The excitation and collection fibers were positioned near the isocenter, ~90° relative to the beam axis. The spot illuminated on the tissue surface was ~5 mm in diameter.

Results

Fast oxygen measurements

A typical trace showing oxygen depletion in solution (20 mM phosphate, pH 7.2, BSA 5%) subjected to sequential exposures of proton FLASH is shown in Fig. 1a. The radiation doses varied (10 Gy, 30 Gy and 100 Gy), but the dose rates for all irradiations were the same, ~110 Gy/s. In all cases, application of FLASH caused fast depletion of oxygen with the magnitude correlated with the total delivered dose. The trace shown in Fig. 1a was recorded with the temporal resolution of 2 Hz, except for the last three irradiation events, where the measurement frequency was 3.33 kHz (300 μs per data point). An expanded view of the depletion step corresponding to the dose of 30 Gy (encircled in Fig. 1a) is shown in Fig. 1b, confirming that application of radiation (total duration ~300 ms) causes a linear decline in O_2. However, the noise in the data recorded at this rate was such that some of the [O_2] values deviated by as much as 60–70 μM. Examination of the decays collected during FLASH revealed that the error was mostly due to random ‘spikes’ (Fig. 1b, inset) inflicted by the radiation. The spikes could be caused by scattered particles or Cherenkov flashes due to the beam microstructure. To eliminate this non-random noise, an algorithm was developed, which automatically detected and removed the ‘spikes’ from the decays (SI, p. S5) prior to fitting. Such filtering alone resulted in a significant boost of SNR ($\delta[O_2]=\pm 5.5$ μM, Fig. 3c) without jeopardizing the measurement rate. Further improvement could be achieved by binning/averaging of the decays after spike removal (Fig. 1d). Although averaging decreased the apparent temporal resolution, the resulting rate of 0.5–1 kHz (1.2 ms per data point in Fig. 3d) was still sufficient for capturing the dynamics during FLASH, far exceeding the rates of all previously reported oxygen measurements.

Oxygen depletion in solutions containing Bovine Serum (BSA) vs diH_2O

To verify that measurements with soluble Oxyphors can report quantitatively on oxygen levels in the presence of ionizing radiation, we compared oxygen depletion by FLASH in solutions containing organic scavengers with depletion in pure water (Fig. 2). These experiments were carried out using Oxyphor PtG4 and then repeated with two other dendritic probes, Oxyphor PdG4[41] and Oxyphor 2P[42] to eliminate potential effects of probe-specific chemistry. Measurements with all probes produced similar results.

Consecutive exposures of the BSA solution to FLASH caused stepwise increases in the phosphorescence lifetime τ (Fig. 2a). The oxygen trace (Fig. 2b (inset)) was derived from the τ-trace. The lifetime in the end of the run reached the value of τ_0=51.5 μs (τ_0 is defined in Fig. 5), matching that obtained in independent experiments, where oxygen was displaced from solutions by inert gas (argon). Additional FLASH exposures had no further effect on τ.

In pure H_2O, the lifetime trace initially exhibited similar stepwise increments (Fig. 2c), however, the value of τ_0 was never reached. Instead, starting at ~47 μs (arrow) the radiation pulses began causing sharp drops in τ, followed by slow recovery periods (half-time ~25 s). The levels to which the lifetime recovered decreased gradually as FLASH exposures continued. Fast recording (Fig. 2c, inset) revealed that the recovery had hyperbolic-like profile, characteristic of second-order processes.

Additional insights were obtained from the traces of the decay initial amplitudes (Fig. 2b,d). The initial amplitude of the phosphorescence decay (I_0, Fig. 5) reflects the size of the triplet population produced by the light pulse. For infinitely short pulses, I_0 should remain independent of the decay lifetime τ and of the presence of quenchers. For excitation pulses of finite duration, a positive correlation between I_0 and τ is expected. In the presence of BSA (Fig. 2b) the time trace of I_0 showed a small rise in parallel with the increase in τ (Fig. 2a). The magnitude of the rise is consistent with the duration of the excitation pulse (5 μs) being shorter than τ everywhere along the trace, confirming that the size of the triplet population remained unchanged, and hence the probe remained stable throughout the experiment.

In contrast, in pure water the initial amplitude at first sharply dropped with each FLASH (Fig. 2d) despite sharp increases in τ (Fig. 2c), suggesting that the probe population was depleted, most likely *via* oxidation of the Pt tetrabenzoporphyrin moiety by $OH^{\bullet}$ radicals or *via* the reduction by $e^{-}_{aq}/H^{\bullet}$. Remarkably, the probe depletion did not continue throughout the experiment, but instead slowed down, and then the probe population began rising with each FLASH (Fig. 2d, inset). It appears as if some species have accumulated in solution and are able to “repair” the probe damaged by radiation.

Oxygen depletion g-values

The oxygen depletion *g*-values were measured as a function of oxygen concentration in buffered solutions of BSA (1%, 2% and 5%) upon exposure to conventional (0.6 Gy/s) and FLASH (~100 Gy/s) irradiation (Fig. 3). Oxygen was depleted in sealed vials in stepwise fashion by applying fixed radiation doses, similar to the experiments shown in Fig. 1a and 2a. The dose rates were kept constant throughout each run.

For both conventional and FLASH dose rates the apparent oxygen depletion *g*-values (Fig. 3a, Fig. S3) were first slightly rising in the range from the air saturation to ~20–30 μM [O_2], but starting from ~20 μM they dropped steeply to zero. The decrease began slightly earlier in the case of FLASH irradiation. The change was reflected in the respective [O_2] *vs* time traces in the low-oxygen region (Fig. 3b). The depletion experiments were repeated using Oxyphors PtG4, PdG4 and 2P, giving similar results. PdG4 due to its longer triplet lifetime (τ_0=270 μs at 22°C) has particularly high sensitivity to small oxygen changes. The graph shown in Fig. 3b was obtained using that probe.

In the [O_2] range of 30–140 μM (pO_2 ~17–60 mmHg), where the *g*-values were relatively constant, the depletion at conventional dose rate was ~0.55 μM/Gy, which is ~13% higher than depletion by FLASH (~0.49 μM/Gy). The ratio was similar for all concentrations of BSA examined (Fig. 3c), echoing the results obtained in the previous studies[38,39] and confirming that even at relatively low concentrations (in the present case starting at ~2%) the concentration of the organic substrate does not affect the rate of the overall oxygen consumption reaction.

In vivo experiments

The probe (PtG4, 20 μL, 100 μM) was delivered directly into the interstitial space of the leg muscle tissue in mice by injection, and the measurements were performed 24h later (see Methods and Materials). The bio-distribution of the dendritic phosphorescent probes, such as PtG4, has been discussed previously.[29,30,41,42]

FLASH induced a rapid decrease in tissue pO_2, followed by a rebound, presumably due to the resupply of oxygen from the blood (Fig. 4a). The recording was performed at 3.33 kHz rate with subsequent peak removal and 5-decays averaging (see above), which effectively reduced the time resolution to one data point per 1.5 ms. The depletion trace appeared to be linear over the irradiation period (~0.3 s), while the rebound had a somewhat wavy profile. The baseline was reached after ~4.8 s, followed by a small overshoot. Neither the wavy profile nor overshoot were present in all experiments, but apparent in more than one case.

The baseline pO_2 levels varied between different animals, presumably due to different responses to anesthesia. An observation was made that the amount of oxygen depleted by FLASH (ΔpO_2) appears to correlate with the baseline pO_2 levels (Fig. 4b).

Discussion

Theoretically, the temporal resolution of the phosphorescence quenching method is defined by the probe's triplet lifetime. In a typical ensemble-type experiment 5–6 lifetimes are usually sufficient to sample a luminescence decay for reliable calculation of its time constant, provided the data can be recorded with adequate signal-to-noise ratio (SNR) after a single excitation pulse. Thus, for probes with lifetimes in the range of tens-to-hundreds of microseconds, which are optimal for physiological oxygen recordings,[30,41,42] a single measurement requires ~10^{-4}-10^{-3} s. However, in practice many (hundreds) decays need to be averaged to increase SNR, bringing the temporal resolution into the sub-second/second range. In the experiments reported herein we took advantage of the high brightness

of Oxyphors and efficient photon detection, which allowed us to obtain high quality phosphorescence decays upon just one excitation pulse. In addition, specialized data processing algorithms were implemented for removing non-random noise (spikes) caused by radiation, increasing fidelity of the lifetime calculations.

The phosphorescence quenching method has been used previously in many biological studies. However, its use in the presence of ionizing radiation is new, and it requires careful analysis of potential interfering factors. A diagram of the processes leading to phosphorescence emission (Fig. 5) indicates that triplet states (T_1) can interact not only with ground state oxygen, O_2 ($X^3\sum g^-$), which in biological systems is by far the most efficient and abundant quencher, but with other quenching species (Q) as well, and their effects on phosphorescence need to be considered. It is also important to mention that singlet O_2 ($a^1\Delta_g$), formed in the quenching reaction (Fig. 5), is a highly reactive species on its own, capable of oxidizing organic matter. However, as shown previously[43] and confirmed in the present study (SI, p. S8), at light intensities employed oxygen measurements do not lead to measurable oxygen consumption.

Upon radiolysis of pure water, oxygen is consumed by its reduction to superoxide $O_2^{\bullet-}$ and/or its conjugated acid, hydroperoxyl radical $HO_2^{\bullet}$, either by electrons e^-_{aq} or hydrogen atoms $H^{\bullet}$ (Fig. 6). Ultimately, the long-lived species that accumulate upon radiolysis are H_2O_2 and $O_2^{\bullet-}/HO_2^{\bullet}$. However, in the presence of organic molecules (RH) the situation is different. $OH^{\bullet}$ oxidizes RH and generates radicals $R^{\bullet}$, which subsequently react with O_2 producing peroxyl radicals $ROO^{\bullet}$. On the other hand, *e*aq and $H^{\bullet}$ can reduce organic substrates, forming anion radicals $RH^{-\bullet}$, which ultimately donate their electrons to O_2. As a result, the accumulating species are organic peroxides ROOH and $O_2^{\bullet-}/HO_2^{\bullet}$.

Potentially, all radicals shown in Fig. 6 can quench triplet states by way of photoinduced electron transfer (PET), since triplet states due to their long lifetimes are particularly prone to photochemical transformations. However, primary radicals (e^-_{aq}, $H^{\bullet}$ and $OH^{\bullet}$) are extremely short-lived and never reach appreciable concentrations, while radicals $R^{\bullet}$ and $ROO^{\bullet}$ derived from bio-organic molecules are large, and their diffusion rates are very low. Furthermore, the structures of the Oxyphors[30,41] are such that large macromolecular radicals ($R^{\bullet}$ or $ROO^{\bullet}$) cannot experience direct contacts with triplet chromophores, which are protected by dendrimers. Therefore, the only species that can substantially interfere with phosphorescence are superoxide/hydroperoxyl radical ($O_2^{\bullet-}/HO_2^{\bullet}$) and hydrogen peroxide (H_2O_2).

To evaluate the effect of H_2O_2 on phosphorescence of Oxyphor PtG4 we carried out SternVolmer-type quenching experiments (SI, p. S6), which revealed that quenching of phosphorescence by H_2O_2 in pure water is ~80 times less efficient than by oxygen, while in the presence of BSA no quenching by H_2O_2 could be observed at all, confirming that H_2O_2 has practically no effect on oxygen measurements. In agreement with this result, in the presence of BSA the phosphorescence lifetime τ in the end of oxygen depletion runs (Fig. 2a) matched τ_0, showing that phosphorescence indeed provides a quantitative signal for oxygen. These experiments also suggested that $O_2^{\bullet-}$ and $HO_2^{\bullet}$, which are likely to be able to

quench phosphorescence (see below), become fully consumed, presumably in the reduction of peroxyl radicals $ROO^{\bullet}$ (Fig. 6).

In pure water the situation is different. First of all, lifetime τ_0 was never reached (Fig. 2c), indicating that some quenching species always remain present in solution. Furthermore, the dips in τ towards the end of the run reveal that the radiation pulses generate, rather than remove, quenching species. Oxygen formed upon oxidation of superoxide (Fig. 6) could be one of them, but it is unlikely to be the main quencher, since after each pulse τ gradually returned to its pre-pulse value, whereas O_2 is a stable molecule. Since H_2O_2 is not capable of efficient quenching, the most plausible candidates are $O_2^{\bullet-}/HO_2^{\bullet}$. Indeed, the reduction potentials of Pt and Pd tetrabenzoporphyrins and their triplet energies[44] are such that an excited probe is capable of oxidizing $O_2^{\bullet-}/HO_2^{\bullet}$ by way of photoinduced electron transfer.

Analysis of the traces of phosphorescence initial amplitudes (Fig. 2b,d) further confirms that in the presence of organic molecules (e.g. BSA) the probe remains intact and oxygen measurements are quantitative. In contrast, in pure water radiation pulses appear to destroy the probe (Fig. 2d). It is important to emphasize, however, that depletion by itself does not affect oxygen measurements. Decay time τ is independent of the size of the triplet population, but is a function only of the concentration of quencher. As long as some probe remains present, its phosphorescence lifetime correctly reflects the presence of the quenching species.

The fact that in pure water the target for $OH^{\bullet}$ (and/or $e^{-}_{aq}/H^{\bullet}$) was the probe itself, but in the presence of BSA the probe was fully spared implies that nearly all primary radicals are consumed in reactions with BSA, as opposed to entering secondary reactions (Fig. 6), supporting the notion that pure water is significantly different from the biological milieu with respect to oxygen depletion and should not be used as a model medium for studying effects of FLASH on biological systems.[21]

A highly unusual feature, which calls for a separate photochemical investigation, is the apparent regeneration of the probe by radiation pulses towards the end of the depletion run (Fig. 2d). This behavior suggests that the probe's chromophore was not fully destroyed by radiation, but instead converted into some optically silent form, from which it then reappeared. As a speculation, it is possible that Pt(II) porphyrin was oxidized to non-phosphorescent Pt(IV)[45] porphyrin and then reduced back by $HO_2^{\bullet}/O_2^{\bullet}$, as these species accumulated in solution.

Measurements of oxygen depletion *g*-values (Fig. 3) confirmed a previously seen trend: lesser depletion at ultrahigh dose rates than at conventional rates, which has been attributed to the higher rates of self-quenching reactions of the primary radicals along particle tracks. In our case the difference was ~13%, but it is expected to be dependent on the chemistry of the scavenging system and possibly of the dose rate.

An unexpected feature of the plot shown in Fig. 3a is the pronounced oxygen dependence of the g-values in the low O_2 region. To gain insight into this behavior we carried out simulations using the homogeneous kinetic modeling approach[16] (see SI, p. S9), which can be instrumental for understanding the interplay between the rates of individual processes

and experimental observables. In the present case, the main goal of the simulations was to rationalize the oxygen dependence of *g*values. Notably, a recent simulation using the Monte-Carlo approach[40] revealed similar oxygen dependencies, however the dose rates and time scales were significantly different and not directly comparable to our results.

The simulations showed that the *g*-value profile (Fig. 3a) is defined primarily by the rate of reaction of radicals ($R^{\bullet}$) with O_2 (Fig. 6). A lower than diffusion-limited constant for this process, 10^6-10^8 $M^{-1}s^{-1}$,[22] could be assumed based on the large size of the substrate (BSA) and impeded diffusion of oxygen through the folded protein to reach the radical site, assuming that it migrated into the protein interior. For fitting of our data, a rather low value of 5×10^6 $M^{-1}s^{-1}$ was required. While we could not find literature values for rate constants specifically for oxidation of BSA-centered radicals by oxygen, measurements of similar diffusion-limited reactions of triplet states buried inside proteins suggest that such rate constants indeed can be quite low, ~10^7 $M^{-1}s^{-1}$.[46]

The observed oxygen dependence was still surprising in view of the generally very high reactivity of organic radicals toward O_2. Hence, we took care to reproduce the observed effect using different phosphorescent probes. We also considered a possibility that the apparent decrease in oxygen quenching at lower O_2 concentrations could be caused by the concomitant rise of some other quenching species. However, this hypothesis was inconsistent with the observation that in the end of each run the phosphorescence lifetime matched τ_0 for each respective probe.

It is worth a note that in the previous study employing electron FLASH[38] no apparent oxygen dependence of *g*-values was observed. However, the measurements in that case were performed differently: individual solutions with different oxygen concentrations were subjected to a single FLASH, so that no products of radiolysis accumulated in solution. On the other hand, the experiment with protons reported in ref. [39] was performed in a closed system similar to ours, and it did reveal pronounced curvature in the depletion trace as oxygen approached zero. Reconciling the results of these observations and determining the origin of the oxygen dependence clearly requires additional studies and accurate matching of the conditions.

An additional detail that emerged from the fast recordings was that rapid oxygen depletion due to FLASH was followed by a ‘tail’ (Fig. 3b, inset), presumably reflecting gradual decline in quenching species (time constant t_0~2 s). It is possible that this slow after-FLASH phase is a result of non-uniform deposition of energy throughout the volume, followed by equilibration due to diffusion.

Oxygen tracking with high temporal resolution *in vivo* should be able to definitively answer the question whether a hypoxic state is achieved when a clinical radiation dose is delivered at an ultrahigh rate. Here we present only the initial demonstration of *in vivo* recordings (Fig. 4), while leaving a detailed study for the subsequent account. Our initial measurements, however, leave no ambiguity regarding the pO_2 profile during application of FLASH and confirm that a single radiation dose (in this case 30 Gy) delivered at a rate of 100 Gy/s to normally oxygenated tissue does not induce hypoxia.

Unlike in the previous experiments, where the probe was delivered systemically,[38] in the present case Oxyphor PtG4 was confined to the interstitial space. Dendritic probes cannot freely diffuse across vascular walls, and hence the measurements were not directly affected by signals from the probe contained within the vasculature. The ΔpO_2 value of ~8 mmHg (11.4 μM) (Fig. 4a) is more than two times larger than reported previously for electron FLASH (ΔpO_2=2.3 mmHg or 3.27 μM for 20 Gy),[38] which is likely a result of the different probe localization, non-equivalent measurement geometries, oxygen heterogeneity and complex profiles of photon propagation through the tissue. In addition, high sampling rate in the present case made detection of the end point in the depletion trace more accurate. Previously, the first data point could be obtained only ~0.5 s after FLASH, and the ΔpO_2 value could be diminished due to the partial resupply of oxygen.[38]

The observed correlation between the baseline oxygen values and the amount of oxygen depleted by FLASH (Fig. 4b) is consistent with the *g*-value dependencies measured *in vitro* (Fig. 3a) and suggests a possible alternative explanation of the FLASH effect. One can hypothesize that *in vivo* the oxygen consumption *g*-value plots for conventional and FLASH RT are such that the difference between the curves monotonically vanishes as they approach zero (Fig. 4d). If tissue damage is correlated with the amount of oxygen consumed - a hypothesis based on the consideration of the chemistry underlying the oxygen enhancement effect, i.e. O_2 is spent in irreversible reactions of bio-macromolecular radicals (e.g. DNA$^\bullet$), "fixing" the radiation damage (see Fig. 6), - then larger differences between conventional and FLASH RT at normoxic *vs* hypoxic O_2 values are consistent with the FLASH effect as depicted in Fig. 4c. Oxygen consumption during conventional RT does occur *in vivo*, but unfortunately its assessment is obstructed by the resupply of oxygen from the blood,[38] calling for a method for measuring not freely diffusing oxygen molecules, but oxygen that was actually consumed, i.e. chemically bound in reactions with radicals.

Conclusions

The developed variant of the phosphorescence quenching method enables oxygen measurements with rates reaching several kHz. To illustrate the potential of the method we analyzed its performance in the context of FLASH RT, showing explicitly that oxygen depletion upon application of a single clinical radiation dose (30 Gy) to well-oxygenated tissue does not result in the state of tissue-wide hypoxia. Furthermore, our measurements imply that the FLASH effect potentially could stem in part from the difference in the oxygen dependencies of the oxygen consumption *g*-values for conventional *vs* FLASH irradiation. Aside from measurements at ultrafast rates, our analysis shows that the phosphorescence quenching method can be used alongside ionizing radiation for quantitative non-invasive monitoring of tissue oxygenation during therapy.

Supplementary Material

Refer to Web version on PubMed Central for supplementary material.

Acknowledgements

Support of the grants HL145092 (MEK), EB027397 and EB028941 (SAV) from the National Institutes of Health, USA and developmental funds from the Department of Radiation Oncology, University of Pennsylvania Perelman School of Medicine is gratefully acknowledged.

References

1. Dewey DL, Boag JW. Modification of the oxygen effect when bacteria are given large pulses of radiation. Article. Nature. 1959;183(4673):1450–1451. doi:10.1038/1831450a0 [PubMed: 13657161]
2. Michaels HB, Epp ER, Ling CC, Peterson EC. Oxygen sensitization of CHO Cells at ultrahigh dose rates - prelude to oxygen diffusion studies. Article. Radiat Res. 1978;76(3):510–521. doi:10.2307/3574800 [PubMed: 569880]
3. Ewing D. Breaking survival curves and oxygen removal times in irradiated bacterial spores. Letter. Int J Rad Biol. 1980;37(3):321–329. doi:10.1080/09553008014550371
4. Hughes JR, Parsons JL. Flash radiotherapy: current knowledge and future insights using proton-beam therapy. Int J Mol Sci. 2020;21:1–14. doi:10.3390/ijms21186492
5. Wilson JD, Hammond EM, Higgins GS, Petersson K. Ultra-high dose rate (FLASH) radiotherapy: silver bullet or Fool's Gold? Front Oncol. 2020;9:1–12. doi:10.3389/fonc.2019.01563
6. Favaudon V, Caplier L, Monceau V, et al. Ultrahigh dose rate FLASH irradiation increases the differential response between normal and tumor tissue in mice. Science Transl Med. 2014;6:245ra93. doi:10.1126/scitranslmed.3008973
7. Expanding the therapeutic index of radiation therapy by normal tissue protection, 92 British Institute of Radiology (2019).
8. Montay-Gruel P, Petersson K, Jaccard M, et al. Irradiation in a flash: unique sparing of memory in mice after whole brain irradiation with dose rates above 100Gy/s. Radiother Oncol. 2017;124:365–369. [PubMed: 28545957]
9. Diffenderfer ES, Verginadis II, Kim MM, et al. Design, implementation and in vivo validation of a novel proton FLASH radiation therapy system. Int J Radiat Oncol Biol Phys: Elsevier Inc.; 2020. p. 440–448.
10. Beyreuther E, Brand M, Hans S, et al. Feasibility of proton FLASH effect tested by zebrafish embryo irradiation. Radiotherapy and Oncology. 2019;139:46–50. doi:10.1016/j.radonc.2019.06.024 [PubMed: 31266652]
11. Vozenin MC, De Fornel P, Petersson K, et al. The advantage of FLASH radiotherapy confirmed in mini-pig and cat-cancer patients. Clin Cancer Res. 2019;25:35–42. doi:10.1158/10780432.CCR-17-3375 [PubMed: 29875213]
12. Faster and safer? FLASH ultra-high dose rate in radiotherapy, 91 British Institute of Radiology (2018).
13. Al-Hallaq H, Cao MS, Kruse J, Klein E. Cured in a FLASH: reducing normal tissue toxicities using ultra-high dose rates. Editorial Material. Int J Radiat Oncol Biol Phys. Jun 2019;104(2):257–260. doi:10.1016/j.ijrobp.2019.01.093 [PubMed: 31047621]
14. Alaghband Y, Cheeks SN, Allen BD, et al. Neuroprotection of radiosensitive juvenile mice by ultra-high dose rate FLASH irradiation. Article. Cancers. Jun 2020;12(6):21. 1671. doi:10.3390/cancers12061671
15. Spitz DR, Buettner GR, Petronek MS, et al. An integrated physico-chemical approach for explaining the differential impact of FLASH versus conventional dose rate irradiation on cancer and normal tissue responses. Radiother Oncol. 2019;139:23–27. doi:10.1016/j.radonc.2019.03.028 [PubMed: 31010709]
16. Labarbe R, Hotoiu L, Barbier J, Favaudon V. A physicochemical model of reaction kinetics supports peroxyl radical recombination as the main determinant of the FLASH effect. Radiother Oncol. 2020;153:303–310. doi:10.1016/j.radonc.2020.06.001 [PubMed: 32534957]
17. Bourhis J, Sozzi WJ, Jorge PG, et al. Treatment of a first patient with FLASH radiotherapy. Radiother Oncol. 2019;139:18–22. doi:10.1016/j.radonc.2019.06.019 [PubMed: 31303340]

18. Pratx G, Kapp DS. A computational model of radiolytic oxygen depletion during FLASH irradiation and its effect on the oxygen enhancement ratio. Phys Med Biol: IOP Publishing Ltd; 2019.
19. Petersson K, Adrian G, Butterworth K, McMahon SJ. A quantitative analysis of the role of oxygen tension in FLASH radiation therapy. Int J Rad Oncol Biol Phys. 2020;107:539–547. doi:10.1016/j.ijrobp.2020.02.634
20. Adrian G, Konradsson E, Ceberg C, Lempart M, Back S, Petersson K. The FLASH effect depends on oxygen concentration. Brit J Radiol. 2020;93:20190702.
21. Wardman P. Radiotherapy using high-intensity pulsed radiation beams (FLASH): a radiationchemical perspective. Editorial Material. Radiat Res. Dec 2020;194(6):607–617. doi:10.1667/rade-1900016
22. Favaudon V, Labarbe R, Limoli CL. Model studies of the role of oxygen in the FLASH effect. Article; Early Access. Med Phys. 2021:14. doi:10.1002/mp.15129
23. Hall EJ, Giaccia AJ. Radiobiology for the radiologist: 6th (sixth) edition. Lippincott Williams & Wilkins; 2006.
24. Wardman P. Time as a variable in radiation biology: the oxygen effect. Editorial Material. Radiat Res. Jan 2016;185(1):1–3. doi:10.1667/rr14323.1 [PubMed: 26731298]
25. Ling CC, Michaels HB, Epp ER, Peterson EC. Oxygen diffusion into mammalian cells following ultrahigh dose rate irradiation and lifetime estimates of oxygen-sensitive species. Radiat Res. 1978;76:522–532. [PubMed: 734054]
26. Wang XD, Wolfbeis OS. Fiber-optic chemical sensors and biosensors (2015–2019). Review. Anal Chem. Jan 2020;92(1):397–430. doi:10.1021/acs.analchem.9b04708 [PubMed: 31665884]
27. Vanderkooi JM, Maniara G, Green TJ, Wilson DF. An optical method for measurement of dioxygen concentration based on quenching of phosphorescence. J Biol Chem. 1987;262:5476–5482. [PubMed: 3571219]
28. Rumsey WL, Vanderkooi JM, Wilson DF. Imaging of phosphorescence: a novel method for measuring the distribution of oxygen in perfused tissue. Science. 1988; 241:1649–1651. [PubMed: 3420417]
29. Vinogradov SA, Wilson DF. Porphyrin-dendrimers as biological oxygen sensors. In: Capagna S, Ceroni P, eds. Designing Dendrimers. Wiley; 2012.
30. Lebedev AY, Cheprakov AV, Sakadzic S, Boas DA, Wilson DF, Vinogradov SA. Dendritic phosphorescent probes for oxygen imaging in biological systems. ACS Appl Materials & Interfaces. Jun 2009;1(6):1292–1304.
31. Wilson DF, Pastuszko A, Digiacomo JE, Pawlowski M, Schneiderman R, Delivoria-Papadopoulos M. Effect of hyperventilation on oxygenation of the brain cortex of newborn piglets. J Appl Physiol. Jun 1991;70(6):2691–2696. [PubMed: 1909316]
32. Friedman ES, Bittinger K, Esipova TV, et al. Microbes vs. chemistry in the origin of the anaerobic gut lumen. Proc Nat Acad Sci USA. Apr 2018;115(16):4170–4175. doi:10.1073/pnas.1718635115 [PubMed: 29610310]
33. Sakadzic S, Roussakis E, Yaseen MA, et al. Two-photon high-resolution measurement of partial pressure of oxygen in cerebral vasculature and tissue. Article. Nature Methods. Sep 2010;7(9):755–U125. doi:10.1038/nmeth.1490 [PubMed: 20693997]
34. Spencer JA, Ferraro F, Roussakis E, et al. Direct measurement of local oxygen concentration in the bone marrow of live animals. Nature. Apr 2014;508(7495):269. doi:10.1038/nature13034 [PubMed: 24590072]
35. Wilson DF, Cerniglia G. Localization of tumors and evaluation of their state of oxygenation by phosphorescence imaging. Cancer Res. 1992;52:3988. [PubMed: 1617675]
36. Apreleva SV, Wilson DF, Vinogradov SA. Tomographic imaging of oxygen by phosphorescence lifetime. Applied Optics. 2006;45(33):8547–8559. [PubMed: 17086268]
37. Cao X, Allu SR, Jiang SD, et al. Tissue pO_2 distributions in xenograft tumors dynamically imaged by Cherenkov-excited phosphorescence during fractionated radiation therapy. Article. Nature Commun. Jan 2020;11(1):9. 573. doi:10.1038/s41467-020-14415-9 [PubMed: 31911596]

38. Cao X, Zhang R, Esipova TV, et al. Quantification of oxygen depletion during FLASH irradiation in vitro and in vivo. Int J Radiat Oncol Biol Phys. 2021;111 (1):240–248. doi:10.1016/j.ijrobp.2021.03.056 [PubMed: 33845146]

39. Jansen J, Knoll J, Beyreuther E, et al. Does FLASH deplete oxygen? Experimental evaluation for photons, protons and carbon ions. Article. Med Phys. Jul 2021;48(7):3982–3990. doi:10.1002/mp.14917 [PubMed: 33948958]

40. Boscolo D, Scifoni E, Durante M, Krämer M, Fuss MC. May oxygen depletion explain the FLASH effect? A chemical track structure analysis. Radiother Oncol. 2021;162:68–75. [PubMed: 34214612]

41. Esipova TV, Karagodov A, Miller J, Wilson DF, Busch TM, Vinogradov SA. Two new “protected” Oxyphors for biological oximetry: properties and application in tumor imaging. Anal Chem. Nov 2011;83(22):8756–8765. doi:10.1021/ac2022234 [PubMed: 21961699]

42. Esipova TV, Barrett MJP, Erlebach E, Masunov AE, Weber B, Vinogradov SA. Oxyphor 2P: A high-performance probe for deep-tissue longitudinal oxygen imaging. Cell Metabolism. January 2019 2019;29(3):736–744. doi:10.1016/j.cmet.2018.12.022 [PubMed: 30686745]

43. Ceroni P, Lebedev AY, Marchi E, et al. Evaluation of phototoxicity of dendritic porphyrinbased phosphorescent oxygen probes: an in vitro study. Photochem Photobiol Sci. 2011;10(6):1056–1065. doi:10.1039/c0pp00356e [PubMed: 21409208]

44. Finikova OS, Troxler T, Senes A, DeGrado WF, Hochstrasser RM, Vinogradov SA. Energy and electron transfer in enhanced two-photon-absorbing systems with triplet cores. J Phys Chem A. 2007;111(30):6977–6990. [PubMed: 17608457]

45. Chen P, Finikova OS, Ou ZP, Vinogradov SA, Kadish KM. Electrochemistry of platinum(II) porphyrins: effect of substituents and π-extension on redox potentials and site of electron transfer. Article. Inorg Chem. Jun 2012;51(11):6200–6210. doi:10.1021/ic3003367 [PubMed: 22621652]

46. Khajehpour M, Rietveld I, Vinogradov SA, Prabhu NV, Sharp KA, Vanderkooi JM. Accessibility of oxygen with respect to the heme pocket in horseradish peroxidase. Proteins-Struct Func Gen. 2003;53(3):656–666.

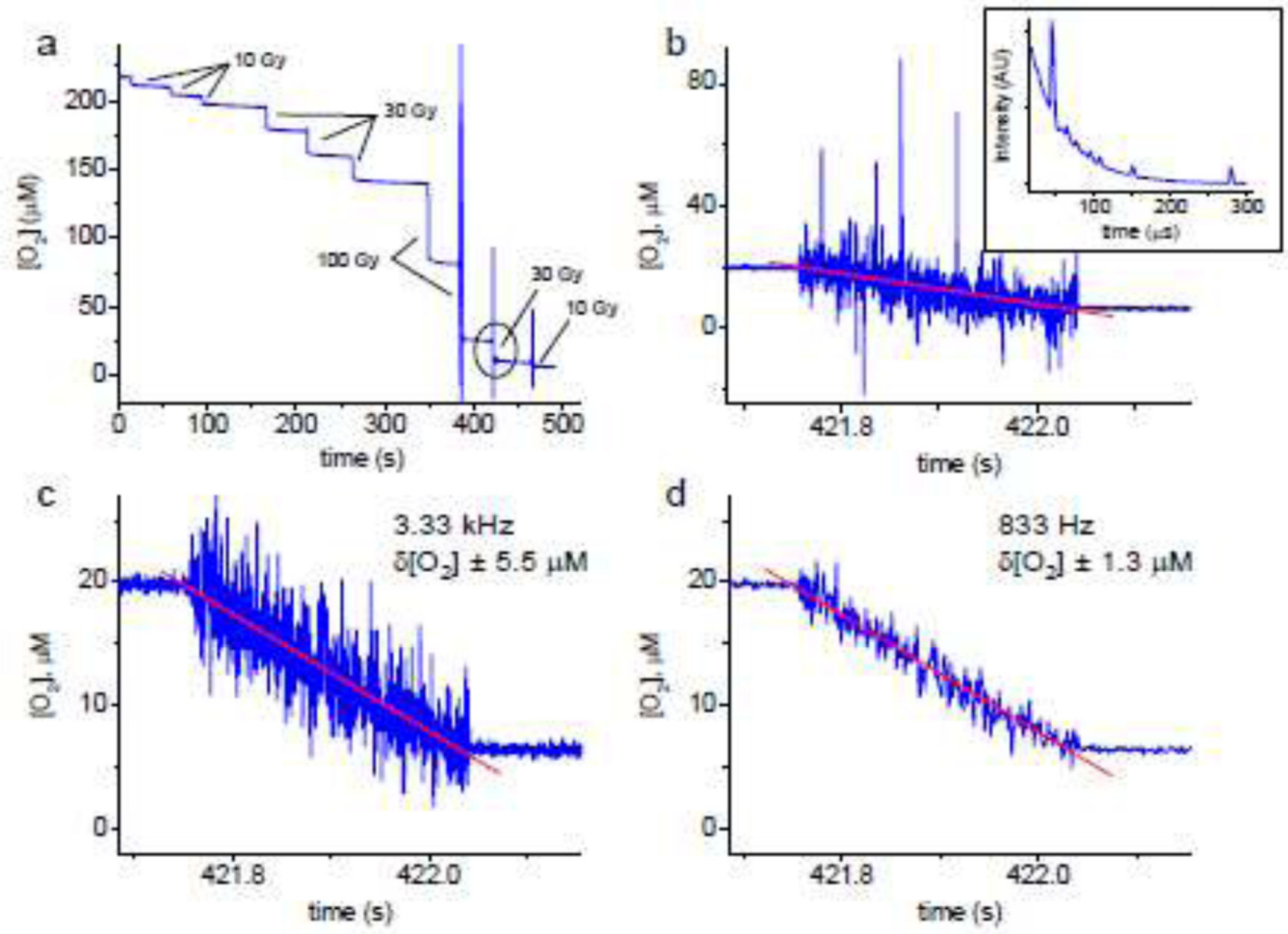

Figure 1.

(a) The time course of oxygen depletion in a sealed vial upon consecutive applications of proton FLASH. Solution: BSA (5% by weight), phosphate buffer (20 mM, pH 7.2), 22°C. Oxygen concentration was measured using Oxyphor PtG4 (1 μM). Dose rate: ~110 Gy/s. The trace is shown starting at lower oxygen concentration than on the ambient air ($[O_2]$~270 mM). (b) Expanded view of the trace encircled in (a), recorded with the time resolution of 3.33 kHz. Inset: a representative phosphorescence decay containing 'spikes' caused by interfering radiation. (c) The same trace after applying the spike-removal algorithm, which reduced the measurement uncertainty $\delta[O_2]$ to ±5.5 μM (δpO_2 ±3.1 mmHg) without jeopardizing the time resolution. (d) Combining spike removal with averaging (four decays) further increases the SNR ($\delta[O_2]$ ±1.3 μM, δpO_2 ±0.73 mmHg), although at the expense of the measurement rate (one data point per 1.2 ms).

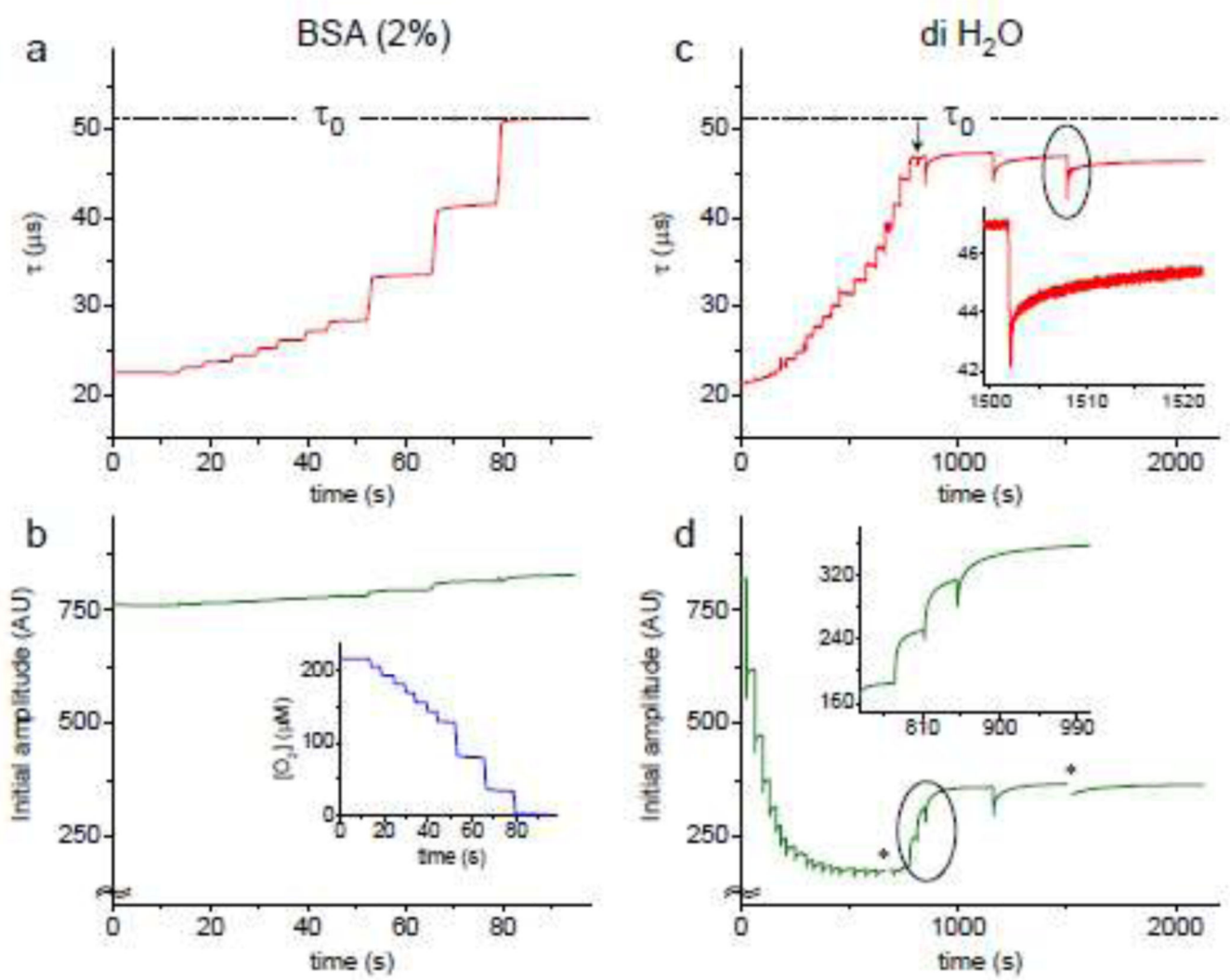

Figure 2.

Changes in the phosphorescence lifetime **τ** (a and c) and phosphorescence decay initial amplitude (b and d) measured in a buffered solution (20 mM phosphate, pH 7.2) containing BSA (2%) (a, b) and in pure water (c, d) at 22°C. Probe: of Oxyphor PtG4 (1 μM). The solutions were subjected to irradiation by proton FLASH: for (a, b) - 7 exposures of 30 Gy, then 3 exposures of 100 Gy; for (c, d) - all exposures were 30 Gy. In all cases, the dose rate was ~105 Gy/s. Inset in (b): [O_2]-trace derived from the **τ**-trace shown in (a). Insets in (c) and (d): expanded sections of the traces encircled in the main graphs. Asterisks in (d) mark the regions corresponding to high-speed recordings, where the determination of the initial amplitudes was obscured by noise.

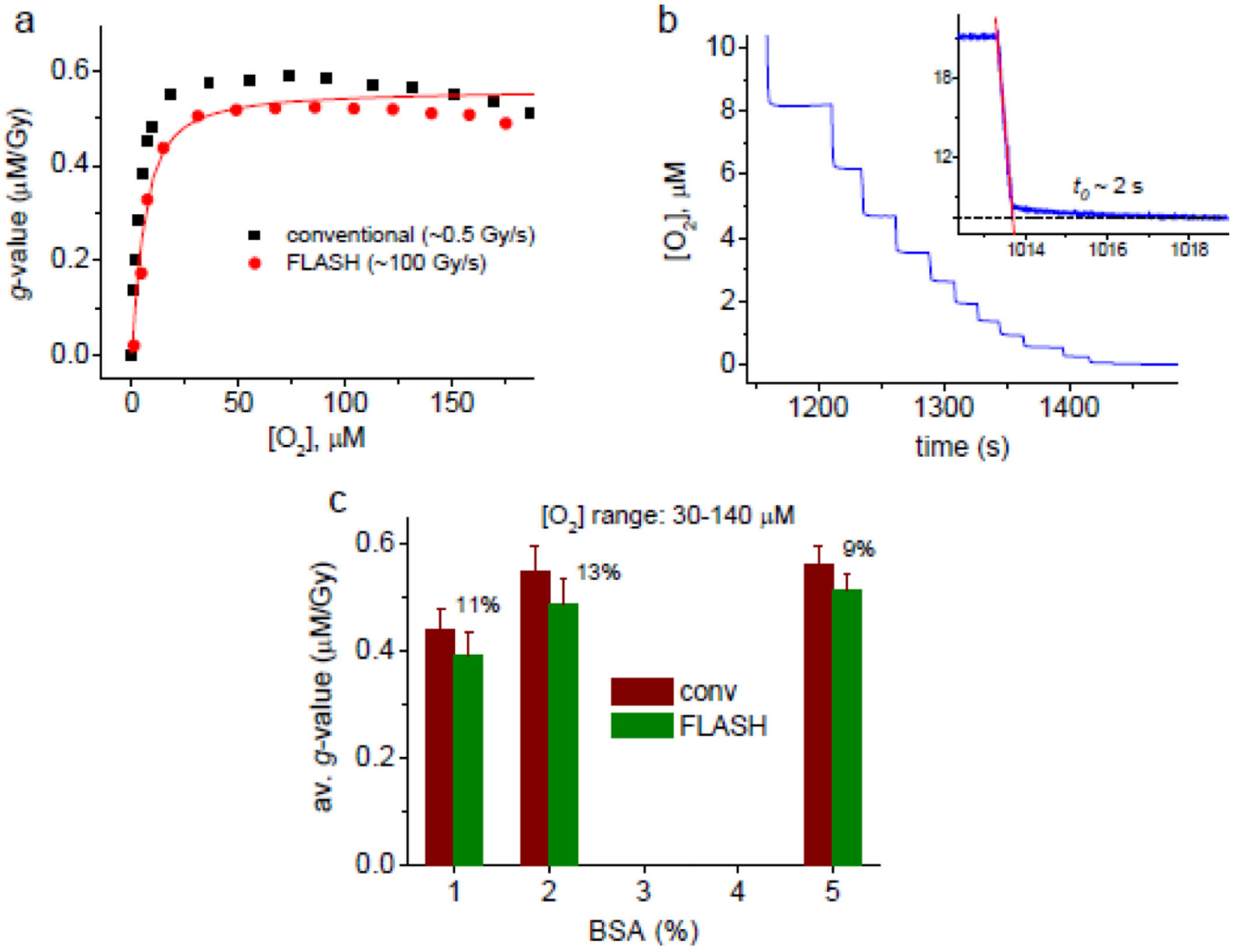

Figure 3.

(a) Oxygen depletion *g*-values (μM/Gy) for conventional and FLASH dose rates (black and red symbols, respectively), in buffered aqueous solutions (5% BSA, 20 mM phosphate, pH 7.2) measured using Oxyphor PtG4. The solid line represents a simulated *g*-value dependence (see text and SI for details). (b) The tail of the oxygen depletion trace for FLASH dose rate (105–109 Gy/s, 10 Gy per FLASH). Measurements using Oxyphor PtG4 and PdG4 produced similar results. Experiments with Oxyphor PdG4 are shown. Inset: depletion of oxygen upon application of FLASH (30 Gy, 100 Gy/s) is followed by a slow decay phase (time constant t_0~2 s). (c) *g*-Values in the range of 30–140 μM for BSA solutions of different concentrations (1%, 2% and 5%).

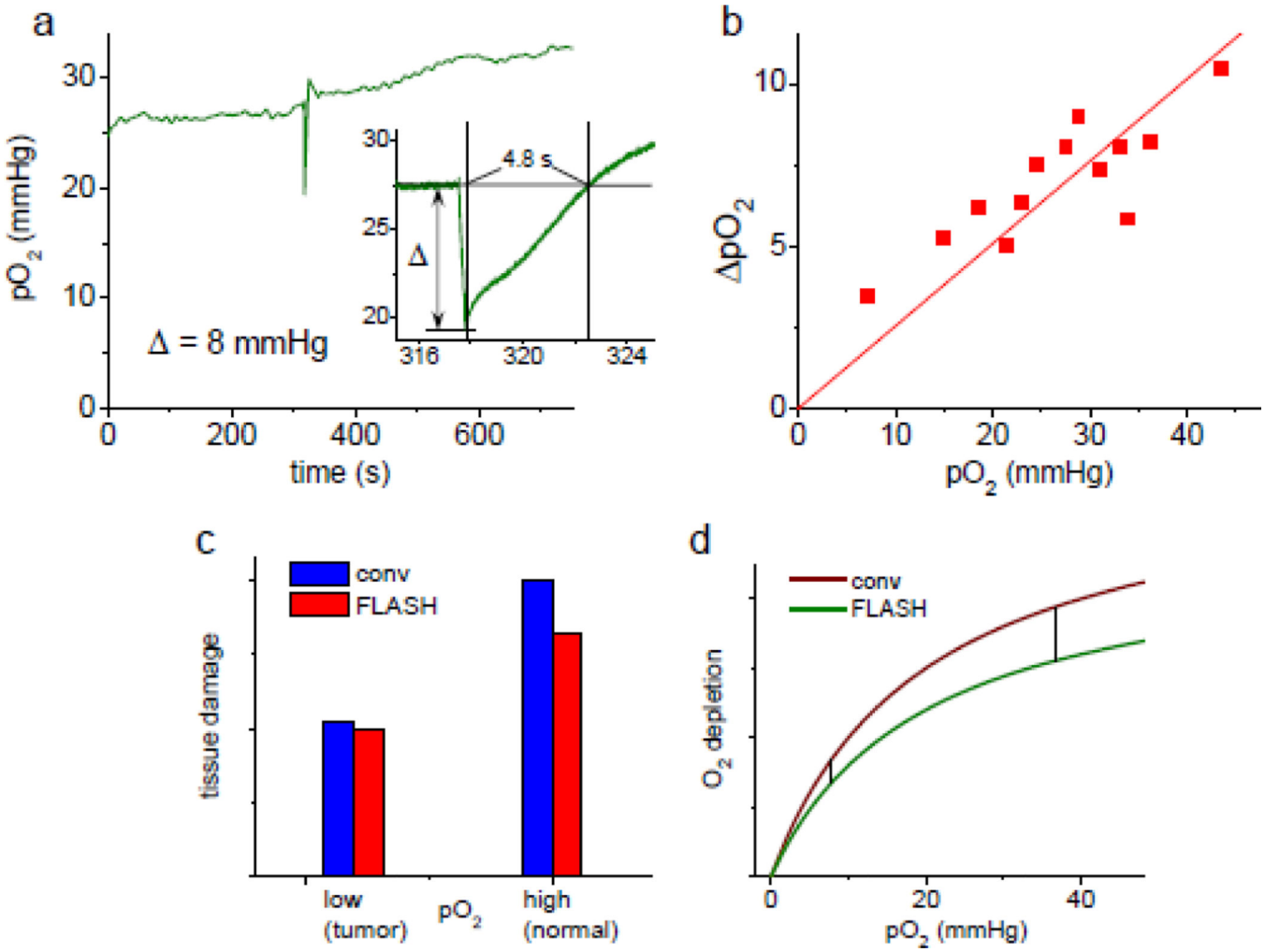

Figure 4.

(a) Trace of extravascular tissue pO_2 in an anesthetized mouse prior to, during and after proton FLASH (30 Gy, 107 Gy/s), measured using Oxyphor PtG4 (20 μL, 100 μM) injected directly into the interstitial space. Inset: changes in pO_2 induced by FLASH measured with the effective rate of 1 data point per 1.5 ms; ΔpO_2=8.03 mmHg (apparent g=0.38 μM/Gy). (b) Correlation between baseline pO_2 and ΔpO_2 for FLASH irradiation (30 Gy, ~100 Gy/s). (c) Graphical representation of the FLASH effect: tissue damage inflicted by FLASH RT is ~20% lower than that by conventional RT for normally oxygenated tissue (normoxia), while for tumor tissue, which is presumed to be hypoxic, the difference between FLASH and conventional RT is negligible. (d) Hypothetical profiles of oxygen consumption g-values for conventional and FLASH RT *in vivo* that potentially could explain the FLASH effect, as depicted in graph (c), assuming that tissue damage is correlated with the amount of oxygen consumed.

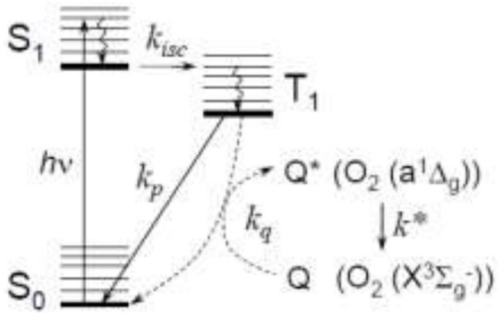

$$\frac{d[T_1]}{dt} = -k_p[T_1] - k_{qO_2}[O_2][T_1] - \left(k_{q1}[Q_1] + k_{q2}[Q_2] + \ldots\right)[T_1] \quad (1)$$

$$I(t) = I_0 \exp(-kt) \quad (2)$$

$$k = \frac{1}{\tau} = k_p + k_{qO_2}[O_2] + \left(k_{q1}[Q_1] + k_{q2}[Q_2] + \ldots\right) \qquad \frac{1}{k_p} = \tau_0 \quad (3)$$

τ – phosphorescence decay time (lifetime).

Figure 5.

Energy diagram illustrating photophysical processes leading to phosphorescence emission and quenching by oxygen (O_2) and other diffusing quenchers (Q_i). Absorption of a photon by an Oxyphor molecule, based on a Pt or Pd porphyrin,[30] is followed by ultrafast $S_1 \rightarrow T_1$ intersystem crossing (*isc*) (k_{isc}=10^{11}-10^{13} s^{-1}), yielding the triplet state (T_1) with nearly unity efficiency. The subsequent $T_1 \rightarrow S_0$ phosphorescence is characterized by the rate constant k_p, the inverse of the phosphorescence lifetime ($1/\tau_0$). The rate equation (1) can be integrated under quasi-stationary approximation, resulting in a single-exponential decay of the phosphorescence intensity $I(t)$ (2), where the rate constant k is defined by the Stern-Volmer relationship (3).

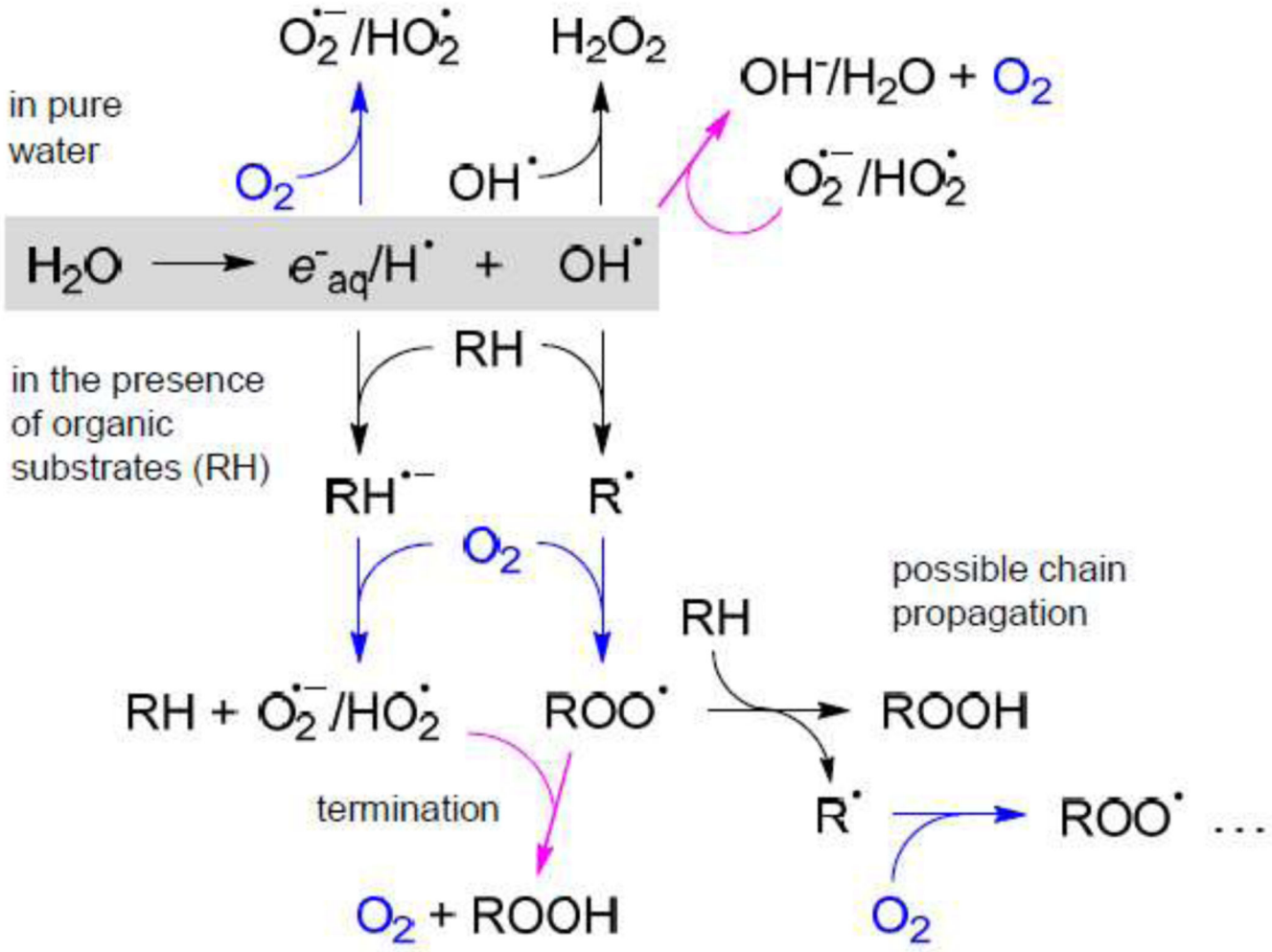

Figure 6.

A simplified scheme of water radiolysis. A number of secondary processes (e.g. radical recombination, superoxide dismutation etc) are omitted in view of their low fluxes under the conditions of our model experiments. Upper part of the scheme: processes occurring in pure water; lower part: processes occurring in the presence of organic substrates (RH). Reactions leading to consumption of oxygen are shown in blue and reactions leading to generation of oxygen are shown in magenta.